

ZEISS Mineralogic Mining

Iron Oxide Analysis by Automated Mineralogy

ZEISS Mineralogic Mining

Iron Oxide Analysis by Automated Mineralogy

Authors: B. Simons BSc PhD
Petrolab Limited, UK

Shaun Graham
Carl Zeiss Microscopy Ltd, UK

Date: November 2015

Distinction between hematite and magnetite using automated mineralogy has long been a difficult task. However, the advent of Mineralogic using a fully quantitative EDS mineral classification methodology, and thus mineral classification by the minerals stoichiometry, has provided a more precise classification of the samples mineralogy. This paper outlines the advantages of using Mineralogic in characterisation of Iron ore samples and discusses the importance of the step sizes required to successfully characterise the fine inter growth textures associated with iron samples.

Introduction

Iron oxide classification by automated mineralogy requires the resolution of several complexities, such as fine-grained intergrowths and subtle variations in chemistry, that are difficult to resolve using traditional optical microscopy. Automated mineralogy techniques can provide a solution to the analysis of iron oxides by using specific instrument settings to resolve mineral chemistry. Fine-grained textures can be resolved using an adequate pixel spacing during analysis.

The problem

Complexities of iron oxide intergrowths in samples such as gossans and Banded Iron Formations (BIFs) are not always easily resolved by use of traditional techniques e.g., reflected light microscopy. However, the identification of different iron oxides (e.g., magnetite, haematite, goethite) by energy dispersive spectroscopy (EDS) is possible with careful consideration of mineral chemistry supported by variations in the back scattered electron (BSE) signal of the different minerals (e.g., Tonžetić and Dippenaar, 2012; Anderson et al. 2014). Analysis of haematite (Fe_2O_3 ; Fe 69.94%, O 30.06%) and magnetite (Fe_3O_4 ; Fe 72.36%, O 27.64%) can be problematic due to their close stoichiometric formulae and chemistry. This example demonstrates that mineral chemistry of haematite and magnetite can be resolved by EDS and investigates the effects of increased pixel spacing, decreased analysis time and decreased fidelity of the data output.

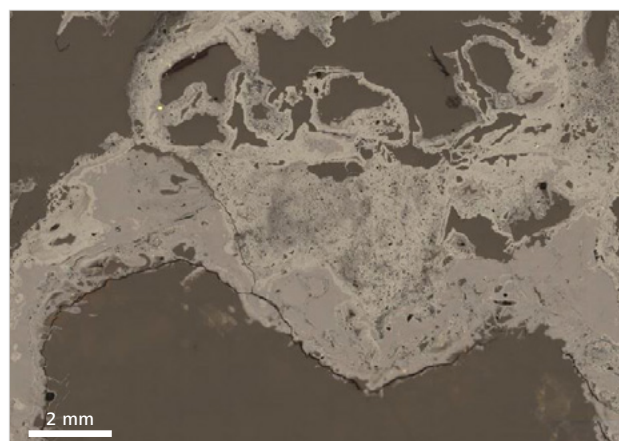


Figure 1 Reflected light image of sample showing fine banded magnetite (brownish grey) and haematite (grey) with gold visible in the top left of the image. Image shows approximate area of automated analysis.

Sample

A sample of a gold-bearing gossan was examined by reflected light microscopy using microscope Axio Imager.Z2m with a 130x85 STEP (D) automated stage and determined to contain variably intergrown and banded iron oxides with coarse gold, biotite micas and quartz (Figure 1).

There are localised areas of very fine-grained intergrown iron oxides ($< 2 \mu\text{m}$) that have a speckled appearance and banded iron oxides with bands of less than $5 \mu\text{m}$ in width.

Coarse gold reaches up to $20 \mu\text{m}$ but is typically $< 5 \mu\text{m}$.

Analytical conditions

One sample of a gold-bearing gossan was prepared as a 30 mm polished block and carbon coated to a thickness of 10 nm. Quantitative mineralogical analysis was conducted on a ZEISS ruggedized MinSCAN scanning electron microscope (SEM) with two Bruker xFlash® 6|30 x-ray detectors and Mineralogic Mining Automated Mineralogy at Petrolab Limited, Redruth, Cornwall. The analysis was carried out using a requested I probe of 1.5 nA, an acceleration voltage of 20 kV and a PB-ZAF matrix correction routine. Standard-less calibration of the EDS detectors was carried out every 90 minutes on a Cu standard (Cu K α peak).

Mineralogic Mining conducts automated analysis using a number of different methods including: mapping, line scan, spot centroid, feature scan and BSE only. For this analysis, mapping was utilised where x-ray spectra are collected at a set magnification and pixel spacing. The pixel spacing, beam dwell time for each pixel and EDS classification using the fully quantitative EDS are defined by the operator. Mineralogic Explorer® 1.2 was used for reviewing data. The overall mineral map containing 57 fields was produced using a magnification of 520 with a 2 μ m spacing. One field of view with an approximate size of 500 x 375 μ m was analysed using the same magnification with 2 μ m, 4 μ m, 8 μ m and 16 μ m spacings to investigate the decrease in analysis time with loss of resolution of the mineral map. The mineralogical classification was determined prior to analysis by calibrating the detectors and determining the

Mineral	Chemistry (weight % per element)	Average composition
Biotite	Si: 7-61, Al: 5-30, Fe: 0.1-40, K: 3.01-14, O: 30-60	Si: 15.4, Al: 10.92, Fe: 35.97, K: 6.5, O: 30.84
Cr-rich haematite	Cr: 3-30, Fe: 30-71, O: 20-50	Fe: 45.96, Cr: 24.12, O: 29.92
Electrum	Ag: >20, Au: <80	Au: 74.07, Ag: 25.93
Gold	Au: >80	Au: 100
Haematite	Fe: 55-71, Si: 0-5, O: 20-50	Fe: 69.94, O: 29.18
Ilmenite	Fe: 25-55, Ti: 27-45, O: 20-50	Fe: 35.69, Ti: 29.23, O: 35.08
Magnetite	Fe: 71.01-90, O: 20-40	Fe: 73.39, O: 25.98

Table 1 Mineral categories and the compositional constraints used in the chemical classification to produce the false colour mineral maps. Except gold and electrum, all also contain oxygen.

compositional parameters from known occurrences of magnetite and haematite within the sample (Table 1). The determined compositions lie close to the stoichiometric compositions. A single field of view was used to refine the mineralogical classification so that the BSE signal and EDS classification were in good agreement.

Solution

Magnetite and haematite can be distinguished by their chemistry which can be resolved by acquiring sufficient count data from the SEM. A dwell time of 0.28 seconds for each pixel was required to resolve the chemistry of the iron oxides. This dwell time resulted in EDS counts per second

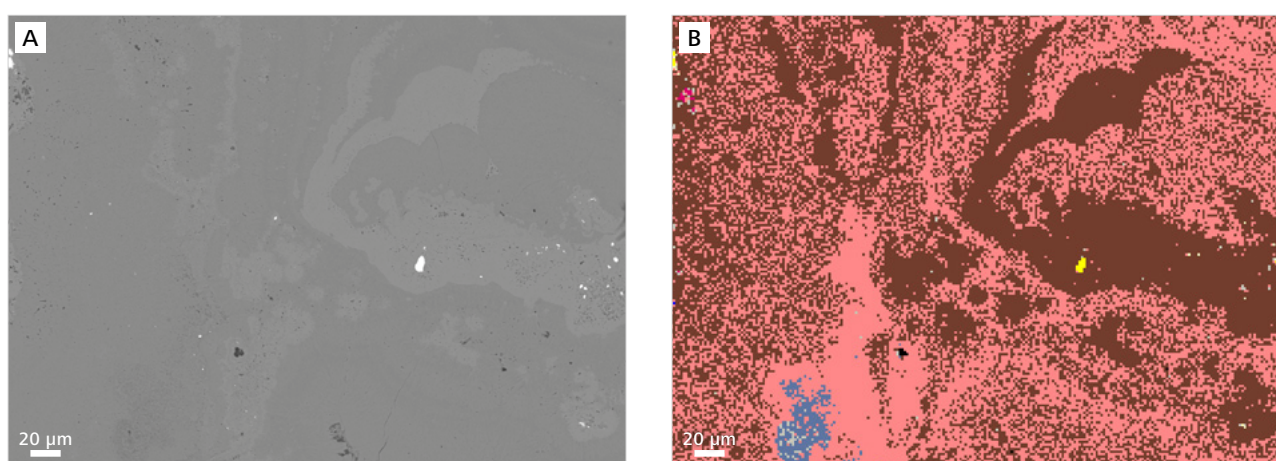


Figure 2 (A) Back scattered electron (BSE) map showing distinction between the BSE signal of magnetite and haematite which is matched by variations in mineral chemistry in (B) the false colour mineral map (2 μ m pixel spacing).

■ Biotite ■ Electrum ■ Haematite ■ Magnetite ■ Cr-rich haematite ■ Gold ■ Ilmenite

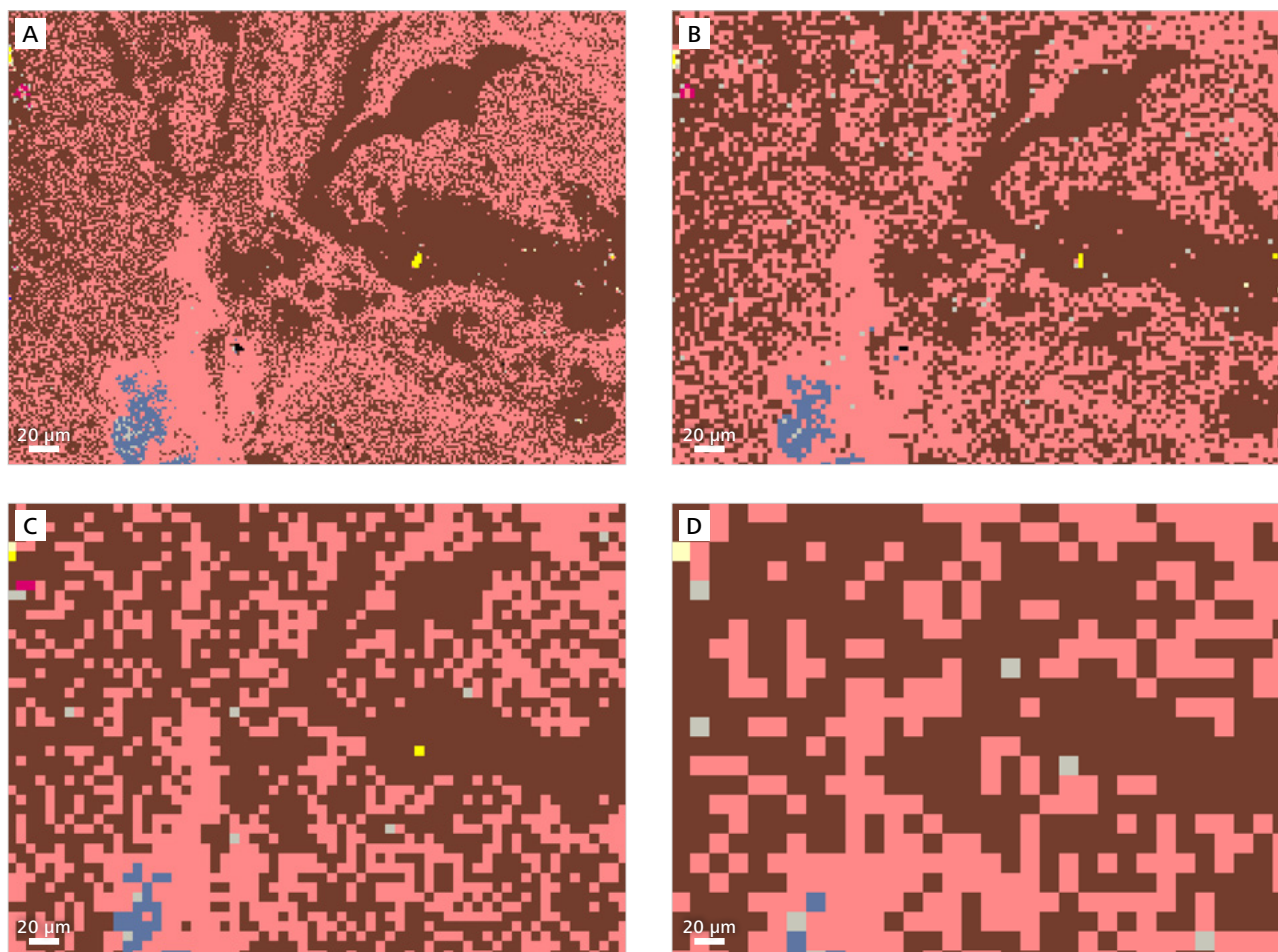


Figure 3 Loss of sample clarity at the same magnification but larger pixel spacing. (A) 2 μm and (B) 4 μm pixel spacing retaining the textures within the samples. (C) 8 μm pixel spacing retains the magnetite texture around the gold (right hand side) but loses the texture elsewhere. (D) 16 μm pixel spacing which is not suitable for analysis of this sample. No textures are preserved and the gold is not detected.

■ Biotite ■ Electrum ■ Haematite ■ Magnetite ■ Cr-rich haematite ■ Gold ■ Ilmenite

(CPS) of over 5000 for gold, approximately 3000 for magnetite and haematite and <2000 for quartz, the mineral with the lowest BSE signal. In this example, variations in the BSE of the sample are mirrored by variations in obtained EDS, with magnetite showing a brighter BSE. This information produced an arbitrary division between the iron oxides that was utilised in classification of the sample. The false colour mineral map closely matches the variation displayed by the BSE map (Figure 2).

Effect of pixel spacing

A disadvantage of increasing dwell time to resolve the iron oxide chemistry is the increased time required for analysis.

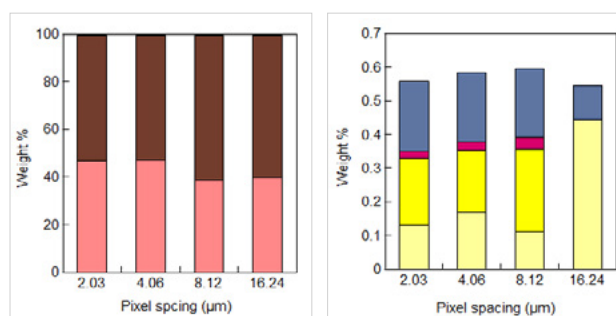


Figure 4 Graphs displaying the effect of pixel spacing on the modal abundance of (A) major iron oxides and (B) accessory minerals.

■ Biotite ■ Electrum ■ Haematite ■ Magnetite
■ Cr-rich haematite ■ Gold ■ Ilmenite

Increasing the pixel size may speed up data acquisition but will result in loss of finesse in the final sample map (Figure 3). For example, analysis of one field of view is 37 times faster using a 16.24 μm spacing compared with using a spacing of 2 μm . There is a distinct loss of detail in the final mineral map when using a larger pixel spacing due to the fine grained textural variation of the sample. The 4 μm spacing retains much of the sample detail compared to the 2 μm spacing and analysis is nine times faster. The bulk modal mineralogy is also affected by the pixel spacing. In this sample, for the 16 μm spacing, there is no detection of gold. This is likely due to the grain size of the gold which is smaller than the step size so it is missed in the analysis. Examination of the sample using reflect light microscopy indicates that the gold is typically <5 μm and so any step size larger than this may result in the gold being missed. For a coarser spacing there are fewer analyses which, in this sample, increases the modal abundance of magnetite (by approximately 5 % modal abundance) at the expense of haematite. There is also no detection of biotite and a reduction in the modal abundance of Cr-rich haematite (Figure 4).

Conclusions

Iron oxide chemistry can be successfully resolved using automated mineralogy by ensuring that dwell times are high enough to obtain sufficient quality spectra to produce accurate quantitative data. High count data enables the separation of mineral chemistry of common iron oxide minerals such as magnetite and haematite, which can be supported by variations in the BSE grey levels of these minerals. Analysis time can be reduced according to the grain size of variations in the sample allowing rapid quantification of iron oxide-bearing samples by EDS or by alteration of the beam parameters.

Operating conditions

SEM	ZEISS MinSCAN
Detector	Bruker xFlash 6130 (two)
SEM software	Mineralogic® Mining 1.2
Analysis software	Mineralogic Explorer 1.2
Filament	Agar A054 tungsten
iProbe	1.5 nA
EHT	20 kV
Fil I Target	2.588 A
Calibration	Cu Ka
BSE signal	Low = 55 (quartz); high = 255 (gold)
Z height	9.228 mm
Scan speed	6
Working distance	18.0 mm
Dwell time	0.28 seconds
BSE image brightness	40.9 %
BSE image contrast	65.6 %

References:

- [1] Anderson, K.F.E., Wall, F., Rollinson, G.K. and Moon, C.J. 2014. Quantitative mineralogical and chemical assessment of the Nkout iron ore deposit, Southern Cameroon. *Ore Geology Reviews*, 62, 25–39.
- [2] Tonžetić, I. and Dippenaar, A. 2011. An alteration to tradition iron-ore sinter phase classification, *Minerals Engineering*, 24, 1258–1263.



Carl Zeiss Microscopy GmbH
07745 Jena, Germany
microscopy@zeiss.com
www.zeiss.com/microscopy



Not for therapeutic, treatment or medical diagnostic evidence. Not all products are available in every country. Contact your local ZEISS representative for more information.

EN_42_013_188 | CZ 03-2016 | Design, scope of delivery and technical progress subject to change without notice. | © Carl Zeiss Microscopy GmbH